Model Development, Field Section Characterization and Model Comparison for Excess Vehicle Fuel Use Due to Pavement Structural Response

By

Erdem Coleri, Ph.D. *(corresponding author)*
School of Civil and Construction Engineering
Oregon State University
101 Kearney Hall
Corvallis, OR, 97331
Ph: (541) 737-0944, Fax: (541) 737-3052
Email: erdem.coleri@oregonstate.edu

John T. Harvey, Ph.D., P.E.
University of California Pavement Research Center
Department of Civil and Environmental Engineering
University of California, Davis
One Shields Avenue
Davis, CA, 95616
Ph: (530) 754-6409, Fax: (510) 665-3562
Email: jtharvey@ucdavis.edu

Imen Zaabar, Ph.D.
Department of Civil and Environmental Engineering
Michigan State University
428 S. Shaw Lane
East Lansing, MI, 48824
Email: zaabarim@egr.msu.edu

Arghavan Louhghalam, Ph.D.
Department of Civil and Environmental Engineering
Massachusetts Institute of Technology
77 Massachusetts Avenue
Cambridge, MA, 02139
Email: arghavan@mit.edu

Karim Chatti, Ph.D.
Department of Civil and Environmental Engineering
Michigan State University
428 S. Shaw Lane
East Lansing, MI, 48824
Ph: (517) 355-6534
Email: chatti@msu.edu

Transportation Research Board 95th Annual Meeting, Washington, D.C., January 2016.
Total Words (7,643): Text (5,393) + Figures/Tables (2,250 [6 figures + 3 tables])

ABSTRACT

In this study, consumption of energy due to pavement structural response through viscoelastic deformation of asphalt pavement materials under vehicle loading was predicted for 17 field sections in California by using three different models. Calculated dissipated energy values were converted to excess fuel consumption (EFC) to facilitate comparisons under different traffic loads (car, SUV, and truck) and speeds and different temperature conditions. The goal of the study was to compare the different modeling approaches and provide first level estimates of EFC in preparation for simulations of annual EFC for different traffic and climate scenarios as well as different types of pavement structures on the California state highway network. Comparison of the predicted EFC for all test sections showed that all three models produced different results which can be attributed to the differences in the three modeling approaches. However, predictions from the three models are generally of same order of magnitude or an order of magnitude different indicating that overall these models can be calibrated using data from field measurements, which is the next step in the research program.

INTRODUCTION

Pavement Related Mechanisms Affecting Vehicle Fuel Efficiency

Pavements can influence the fuel efficiency and greenhouse gas (GHG) emissions of vehicles through three mechanisms which together can be called the *pavement related rolling resistance*. Models for these mechanisms are needed for use in pavement decision-making in California. The pavement influences can be summarized as follows (*1*):

1. Consumption of energy through the working of shock absorbers, drive train components, and deformation of tire sidewalls as the wheels pass over deviations from a flat surface with wavelengths up to 50 m in the wheelpath (called roughness)—converting mechanical energy into heat which is then dissipated into the air—and thus requires greater work by the engine. This mechanism is managed by maintaining smoother pavement as measured by IRI. Models for this mechanism are well established and have been empirically validated and calibrated.
2. Consumption of energy through viscoelastic working of the tire rubber in the tire/pavement contact patch as it passes over positive macrotexture of the pavement surface and converts it into heat that is dissipated into the tire and the air. Positive macrotexture is caused by stones or grinding/grooving features protruding above the average plane of the pavement surface. This is typically of lesser importance than roughness for macrotexture levels typical in California, and is determined by design of surface treatments, asphalt and concrete mixes and by concrete surface texturing. Raveling on asphalt surfaces and matrix loss on concrete surfaces can increase macrotexture after construction. Models for this mechanism are well established and have been empirically validated and calibrated.
3. Consumption of energy in the pavement itself through viscoelastic deformation of pavement materials under passing vehicles, primarily heavy trucks, which has also been modeled in terms of the geometric relationship between the shape of the deflected pavement under the wheel and the wheel itself. The significance of this mechanism for different types of pavement, different vehicles and vehicle operations, and climate regions, has not been clearly established. Experiments have shown that *(2)* this mechanism can have a significant effect for slow moving heavy vehicles operating on hot viscoelastic pavement, but the significance for other vehicles and conditions is not yet well verified. Models with different approaches have been developed, but have not been comprehensively compared or validated with direct measurement.

Current Status of Research, Development and Implementation

Models for accounting for the GHG emissions from pavement rehabilitation and maintenance, materials production and construction, and the resulting changes in pavement roughness and macrotexture, have been developed by the University of California Pavement Research Center (UCPRC) and implemented in Life Cycle Assessment (LCA) procedures that are being used to analyze Caltrans practices and may be adapted for use in network and project-level decision-making. Similar LCA models are being developed by a number of other organizations for similar purposes. Models are needed for the use phase of LCA that include the effects of pavements on vehicle fuel use.

The most recent validation of models for roughness and macrotexture effects on vehicle fuel use was performed for the National Cooperative Highway Research Program (project 1-45) by Chatti and Zaabar *(2)* on the World Bank's HDM-4 models. The Michigan State University (MSU) project used instrumented vehicles and a set of pavements in Michigan. It is difficult to measure changes in vehicle fuel use from pavement characteristics, which are typically less than five percent, especially separating pavement effects from the effects of wind, tire pressure, speed, grade, etc. Statistically valid results were obtained in the study by careful selection of their test sections, and extensive testing which includes accounting for weather and pavement surface conditions. Recently developed mechanistic models such as the one developed by Louhghalam et. al. *(16, 17)* that relate pavement surface characteristics to the energy loss in vehicle fuel consumption can thus be used with such field measurements to close this gap.

The MSU study validating the HDM-4 models included both asphalt and concrete surfaced pavements. The results showed statistically significant differences due to pavement structural response between asphalt and concrete pavements for heavy trucks moving at slow speeds under hot temperatures; however the pavements were not well characterized and important parameters were back-calculated rather than measured because the focus of the study was not on pavement type or the effects of structural response on vehicle fuel use. The MSU study did show that the effects on fuel economy of roughness and pavement deflection appeared to be independent.

A number of models have been developed for energy dissipation by the deflection mechanism, including models developed by the Massachusetts Institute of Technology *(3, 4)*, the University of Lyons National School of Public Works of the State (ENTPE, *5*), the Swedish National Road and Transport Research Institute (VTI) *(6)* and Michigan State University. There is active research in the development of these models, and several general approaches are being used by model developers. These studies have typically included only a few pavement test sections and vehicle types and limited climate conditions, and have often had very limited if any characterization of the pavement responses. The MIT model has been used to characterize the Virginia DOT pavement network albeit with very simplified structure, climate and load information (7). The OSU model has been developed for this research study. None of these models have been empirically calibrated.

In summary, the deflection energy dissipation models have not been compared with each other for the range of pavement types, vehicles and climates in California. They have also not been validated with comprehensive field data. This is summed up by a statement from a recent review of pavement rolling resistance prepared by VTI and other MIRIAM partners *(8)*:

The overall conclusion is that pavement stiffness cannot be excluded as an important factor influencing rolling resistance, and should be included in studies in the MIRIAM project. The still open question is as to what extent and under which conditions (temperature, type of pavement and light versus heavy vehicles) stiffness is a major factor to consider.

GOALS AND OBJECTIVES

The major goal of this study is to first compare different pavement structural response energy dissipation models and the results they provide for estimated fuel consumption and GHG emissions for a range of California pavements, vehicles and climates using well characterized and documented test sections (Phase 1a). The model results are to be used in simulations of annual traffic and climate conditions on the same California pavements to estimate the net effect on vehicle fuel use of structural response (Phase 1b), the results of which are presented in (*9*). If the simulation results warrant further investigation, the 2nd phase of the project will empirically verify and calibrate the models developed in Phase I using the results of field measurements on the same sections discussed in this paper with instrumented vehicles following the general approach used by MSU for NCHRP 1-45. This paper presents the results of Phase 1a. Steps followed to achieve the Phase Ia goal are given as follows:

- Evaluate the differences and similarities between the models developed by Oregon State University (OSU), MSU, and MIT.
- Identify pavement test sections spanning the range of pavement structures and climate conditions across California and conduct experiments to characterize pavement material and structural properties for modeling.
- Estimate excess vehicle fuel consumption differences due to pavement deflection for range of California vehicles using the developed models.
- Compare the outputs for the three models and comment on the possible reasons for differences.

EXPERIMENT DESIGN AND SELECTION OF FIELD TEST SECTIONS

A factorial of conceptual test sections was prepared by considering pavement types, surface layer thicknesses, roughness level, and subgrade type (clay or sand). Locations for the conceptual test sections were identified by using the software iVision™ to evaluate Caltrans automated pavement condition survey data and forward looking images and the UCPRC software iGPR to review Caltrans ground penetrating radar data. Selected asphalt surfaced sections analyzed to date are given in Table 1. Additional concrete surfaced sections will be analyzed in the near future.

TABLE 1 Field Tests Sections for Model Development and Fuel Consumption Measurements.

Section	District-Highway-County-Direction-Lane	Pavement[1] and Surface Type	Start PM[2]	End PM	Slope	Soil type[3]	IRI[4] (m/km)	MPD[5] (mm)
PD-07	4-SOL-80-W-1	Composite, thick DGAC surface	30.50	29.20	0.05%	SM	0.80	1.06
PD-08	4-SCL-237-W-3	Composite, DGAC surface	5.08	4.48	-0.03%	ML	1.39	1.00
PD-10	4-SOL-505-S-1	Composite, RHMA-G surface	7.50	6.20	-0.06%	SM	0.98	1.11
PD-11	4-SM-101-S-1	Flexible, old thick DGAC surface	18.50	17.50	0.02%	CL	1.34	1.23
PD-13[6]	3-SUT-113-N-1	Flexible, new DGAC surface	13.00	14.00	0.05%	CL	1.50	0.68
PD-14	4-SOL-113-N-1	Flexible, new DGAC surface	3.00	4.00	-0.41%	CL	3.57	0.80
PD-15	3-SAC-50-E-1	Flexible, old thick DGAC surface	14.20	16.00	0.23%	SM	0.99	1.31
PD-16	10-SJ-120-E-1	Flexible, RHMA-O surface on thick DGAC	11.60	12.60	0.11%	SM	1.03	0.78
PD-18[6]	3-YUB-20-W-1	Flexible, old thick DGAC surface	5.00	4.30	-0.11%	ML	1.34	0.97
PD-19	4-SM-101-S-1	Flexible new DGAC surface	25.70	24.50	0.02%	CL	1.12	0.89
PD-20	10-AMA-16-E	Flexible, RHMA-G surface on old DGAC	0.30	0.90	1.94%	ML	1.48	1.33
PD-21	10-SJ-99-N-1	Flexible, RHMA-G surface on new DGAC	25.70	26.50	-0.02%	CH	1.48	1.33
PD-22[6]	4-SCL-101-N-2	Semi-rigid, RHMA-O surface	3.10	4.00	0.27%	CL	1.21	0.74
PD-23	10-STA-132-W-1	Semi-rigid, RHMA-O surface	25.00	24.00	0.10%	SM	0.99	0.92

Notes: [1]: Composite = asphalt on concrete, Flexible = asphalt on granular, semi-rigid = asphalt on cement treated base. DGAC = dense graded asphalt concrete, RHMA-G and –O = rubberized hot mix asphalt gap- and open-graded, respectively

[2]: PM: postmile

[3]: SM:silty sand; CL:low plasticity clay; ML:low plasticity silt.

[4]: IRI: International Roughness Index

[5]: MPD: Mean profile depth

[6] Test sections with two sub-sections.

MEASUREMENT OF TEST SECTION CHARACTERISTICS

After the selection of test sections, section characteristics were determined by conducting falling weight deflectometer (FWD) tests. Three loads (22.2, 35.6 and 53.4 kN) and two repetitions for each load were applied. These load levels are chosen to simulate the deformation that can be created by light and heavy vehicles. In order to estimate the viscoelastic properties of the non-elastic layers, the full time history of the deflection was collected. An example FWD test result (PD-13 – Day time) for the 35.6 kN load level is given in Figure 1.

Each test section had 100 test points evenly spaced along the sections. For each section, two tests were conducted, one early in the morning (3am to 7am) and the other one in the afternoon (12pm to 3pm) in order to capture the temperature effect.

Temperature data (change in temperature with depth) were collected every 15 minutes at one location at the end of the test sections. When temperature profile data could not be collected due to lane closure limitations, they were estimated from measured surface temperatures using BELLS temperature formulas.

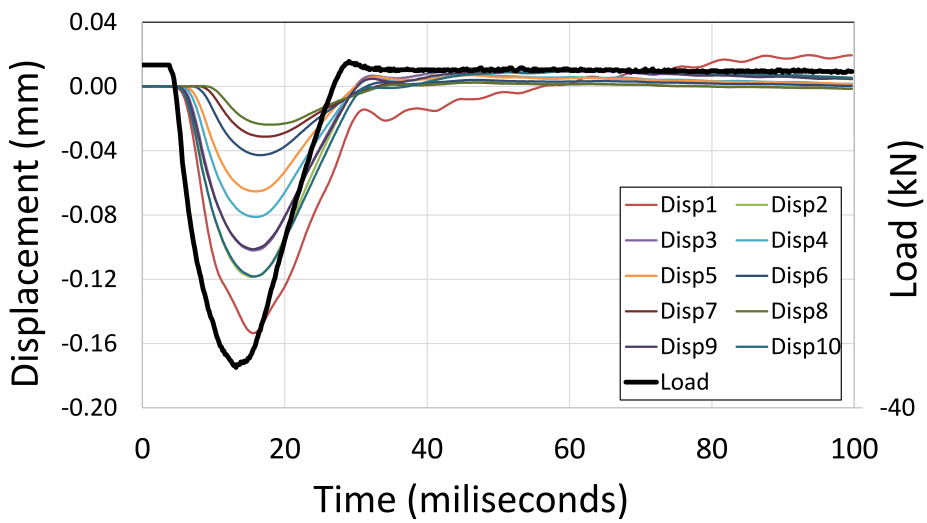

FIGURE 1 Full time history of the deflection data for the estimation of viscoelastic properties.
Note: Sensors are located at the following intervals: sensor1: 0”, sensor2: 8”, sensor3: 12”, sensor4: 18”, sensor5: 24”, sensor6: 36”, sensor7: 48”, sensor8: 60”, sensor9: -8”, sensor10: -12” (Minus sign indicates the other side of the loading plate).

MODEL IMPLEMENTATION AND COMPARISON OF RESULTS

Model Details

Oregon State University (OSU)

A viscoelastic finite element (FE) model was developed to calculate the dissipated energy under different conditions. Energy dissipation due to the subgrade damping is not simulated in the model. In the developed viscoelastic FE model, only the linear behavior is considered (small strain domain). The possible impact of pavement distresses (fatigue, permanent deformations, and cracks) are not taken into account. The material constituting the base is considered isotropic linear elastic.

The temperature dependency of the asphalt mix is defined by using the Williams-Landel-Ferry (WLF) equation, given as follows *(10)*:

$$\log(aT) = \frac{-C_1(T - T_{ref})}{C_2 + (T - T_{ref})} \quad (1)$$

where

aT = the time-temperature shift factor,
C_1 and C_2 = regression coefficients,
T_{ref} = the reference temperature, and
T = test temperature.

To optimize the regression coefficients C_1 and C_2, the shear modulus data were first fitted to a sigmoid function, in the form of:

$$\log(G(\xi)) = \delta + \frac{\alpha}{1 + \exp(\beta + \gamma \log(\xi))} \quad (2)$$

where

α, β, γ, δ = regression coefficients, and
ξ = reduced time.

Shift factors are calculated by fitting the measured or backcalculated modulus to the sigmoidal function (Eqn. 2). One shift factor is calculated at each test temperature while the shift factor for the reference temperature (19^{o}C) is set at zero. A Matlab^{TM} code was developed to optimize the regression coefficients α, β, γ, δ and shift factors for all temperatures. Regression coefficients C_1 and C_2 are calculated by simply fitting the WLF equation to the calculated shift factors.

The generalized Maxwell-type viscoelastic model is used in this study to simulate the time dependency. The model consists of two basic units, a linear elastic spring and a linear viscous dash-pot. Various combinations of these spring and dashpot units define the type of viscoelastic behavior. The implementation procedure developed by Pouget et al. *(5)* is used to simulate the effects of truck loads, vehicle speed, and temperature on dissipated energy.

Abaqus^{TM} software is used for model development. The pavement structure is represented by a 6 m long and 2.5 m wide slab. The finite-element mesh consists of Lagrange brick elements with a second-order interpolation function. The mesh is refined under the wheel path. IRI and macrotexture are not simulated in the model. Therefore the effects of vehicle suspension dynamics on the wheel load are not simulated.

The bottom side of the model is clamped. The symmetry condition in the transversal direction imposes a boundary condition on one side. To ensure the continuity of this slab with the rest of pavement, only vertical displacement is allowed for other lateral sides *(5)*. Perfect bonding is assumed between different pavement layers.

In order to simulate moving wheel loading in the viscoelastic FE model, the trapezoidal impulsive loading method (quasi-static) is used *(11)*. The tire is assumed to have a square contact area and the distribution of load on the tire is assumed to be constant.

The dissipated energy per time w(t) is integrated on a Δd long slice of the asphalt layer, located in the center of the 6 m long structure. It is obtained at any time as the wheel passes. The dissipated energy for a truck (W_{truck}) with Z dual wheels, covering a distance of X can be calculated using the following equation *(5)*:

$$W_{\mathrm{truck}} = \left(\int \mathrm{w(t).dt}\right).\frac{\mathrm{X}}{\Delta \mathrm{d}}.\mathrm{Z} \tag{3}$$

Where w(t) is calculated using the following equation in which ϕ_E is the phase angle, σ_{0z} is the stress curve for the loading time while ε_{0z} is the strain for the same loading time for a unit volume *dV*:

$$W = \iiint (\pi.\sin(\phi_E).\sigma_{0z}.\varepsilon_{0z}).dV$$

Massachusetts Institute of Technology (MIT)

Excess fuel consumption (EFC) due to deflection-induced pavement-vehicle interaction (PVI) is calculated from the energy dissipation a moving load generates within the pavement structure *(3, 4)*. EFC is defined in this paper as the additional fuel consumption compared with a pavement that has no structural response. The model relates pavement material and structural properties to the rolling resistance due to pavement deflection. The pavement is modeled as a viscoelastic beam on an elastic foundation subjected to a moving load at constant speed. To maintain this speed, extra power is provided by the vehicle to compensate for the dissipated energy δE due to viscoelastic deformation of the beam, leading to EFC. The deflection-induced PVI model calculates the excess energy consumption as a function of vehicle speed *c*, axle load $\boldsymbol{P}$, and temperature and material dependent relaxation time $\tau(T)$ as *(3,4)*:

$$\delta E = \frac{c_{cr}}{c} \times \frac{P^2}{bk\ell_s^2} \times F\left(\frac{c}{c_{cr}}; \frac{\tau(T)c_{cr}}{\ell_s}\right) \tag{4}$$

where δE is the dissipated energy per distance travelled due to the pavement deflection as a function of two dimensionless numbers, one related to the vehicle speed, c/c_{cr} (where c_{cr}=l_s sqrt{k/m}), the other to the relaxation time of the pavement material capturing the viscoelastic nature of the top layer $(\tau(T)\ c_{cr})/\ell_s$, with $\ell_s = (\frac{Eh^3}{12}/k)^{1/4}$ the Winkler length of the beam on elastic foundation with width b, top layer modulus E, top layer thickness h, and elastic subgrade modulus k. It is worth noting that the dissipated energy relates to the square of vehicle load,$\delta E \propto P^2$, and the inverse of vehicle speed $\delta E \propto \sim 1/c$. Meanwhile, an increase in temperature results in a reduction in the complex modulus of the viscoelastic top layer, leading to an increase in the dissipated energy. The variation in pavement material properties due to temperature is modeled and calculated separately for asphalt and concrete pavements.

The time-temperature superposition principle is used to establish the temperature dependence of the asphalt and find the material relaxation time at any given temperature T from the relaxation time, measured at a reference temperature T_{ref}:

$$\tau(T) = a_T \times \tau(T_{ref}) \quad (5)$$

where a_T is the shift factor calculated from the Arrhenius law for concrete pavements *(12)*:

$$\log a_T(T) = U_c \left[\frac{1}{T} - \frac{1}{T_{ref}}\right] \quad (6)$$

and from the William-Landel-Ferry equation for asphalt pavements (Eqn. 1) *(10)*:

This results in variation of dissipation due to changes in temperatures and vehicle speeds, and therefore the resulting fuel consumption due to PVI. Note that the characteristic relaxation time and constants C_1 and C_2 are obtained from the back-calculated master-curves.

To simplify the numerical calculations and make them more appropriate for fast computations, the MIT approach uses a fit of the log of dimensionless expression of dissipation to a two-dimensional surface, adapted from Louhghalam et al. *(4)*:

$$\log_{10}\frac{\delta E \ell_s^2 bkc}{P^2 c_{cr}} = \log_{10} F\left(\Pi_1 = \frac{c}{c_{cr}}; \Pi_2 = \zeta = \frac{\tau c_{cr}}{\ell_s}\right) = \sum_{i=0}^{i=5}\sum_{j=0}^{j=3} p_{ij}{\Pi_1}^i \times \log_{10}(\Pi_2)^j \quad (7)$$

Having the material and structural properties of a pavement in hand (a 4 by 6 matrix of 24 model coefficients), one can use Eq. 7 to readily evaluate the dissipated energy and fuel consumption.

Michigan State University (MSU)

Similar to the MIT approach, the MSU approach assumes that the slope in the deflection basin is a grade against which the wheel moves, except that the deflection basins are calculated using a time domain viscoelastic dynamic solution (ViscoWave II – M) instead of the beam on Winkler foundation model. This can then be used to estimate the effect as an additional gradient force that the vehicle has to overcome. The combined effect of damping and vehicle velocity creates a resistive force by putting the vehicle on an uphill slope. This slope adds to the forces resisting vehicle movement through the gradient force, which is related to the instantaneous fuel consumption. Therefore, the dissipated energy calculation consists of calculating the slope in the deflection basins and inputting it as an additional gradient force. The total dissipated energy (J/km) is calculated as:

$$W_{truck} = 1000 \times \sum_{i=1}^{X/\Delta x} \left(P \times G_i \times \Delta x \right) \quad (8)$$

Where P is the vehicle weight and G_i is the slope per unit distance and X is the tire-pavement contact area. Same equation is also used for calculating dissipated energy for the MIT model.

The governing equations for viscoelastic wave propagation used in the MSU approach are similar to any other wave propagation problems; the proposed solution begins with the classical equation of motion for a continuous medium given as the following:

$$(\lambda + \mu) * \nabla(\nabla \cdot \mathbf{u}) + \mu * \nabla^2 \mathbf{u} = \rho \ddot{\mathbf{u}} \quad (9)$$

Similar to the spectral element solution provided by Al-Khoury et. al. *(14)*, a cylindrical axisymmetric coordinate system is used. The solution to the wave equations presented above can be worked more conveniently by utilizing the integral transforms, namely the Laplace and Hankel transforms.

For the moving load formulation the solution to the above equation was used to calculate the response due to a moving load at a given speed and under constant temperature conditions. Only the Hot Mix Asphalt (HMA) modulus was assumed to be time dependent, while the moduli of all other layers and the Poisson’s ratio of all layers (including that of the HMA) were assumed to be time-independent. Axle movements were simulated by sequentially loading and unloading the pavement surface at different points located along the line of travel. A total of 63 points were used to yield 63 unit response time functions at different offset distances. These offsets ranged from -76 in. (1.93 m) to +76 in. (1.93 m) relative to the evaluation point, with 31 points before (approaching) the evaluation point, 31 points after the evaluation point, and one additional point exactly in line with the evaluation point. This 152 in. (3.86 m) long section was required to simulate the complete relaxation under all vehicle loads for all temperatures and speeds. Spacing of these points ranged between 4 in. (101.6 mm) to 1.0 in. (25.4 mm) with denser spacing closer to the evaluation point. A triangular loading shape was applied at each of the loading points. This was done in such a way that the pavement system always carried the full load of the half-axle. As a point on the pavement was loaded, the previous (adjacent) point was unloaded. When the peak load was reached at a given loading point, the load was completely removed from the previous loading point that same instant. Subsequently, all the responses were shifted and summed to obtain the vertical deflection at the evaluation point due to a moving vehicle.

General model assumptions are given as follows:

- Axisymmetric
- Finite layer in the vertical direction (one layer per material type, and continuous mass formulation within the layer element)
- Infinite layer in the horizontal direction (semi-analytical solution)
- Semi-infinite half-space element for the subgrade
- Can accommodate a stiff layer at finite depth

Model Implementation

FWD test results were used to determine unbound layer stiffnesses and to develop relaxation modulus master curves to use for modeling, with the complete time histories of FWD test results used to incorporate phase angle into the process.

The dynamic viscoelastic back-calculation program (DYNABACK-VE) developed as part of the FHWA DTFH61-11-C-00026 project *(15)* was used to back-calculate the master curve E(t) for the asphalt layers using the time histories of FWD sensor deflections at different temperatures. The method uses a time domain viscoelastic solution as a forward routine (ViscoWave-II) and a hybrid routine (DYNABACK-VE) using a genetic algorithm and modified Levenberg-Marquardt method) for back-calculation analysis. The advantage of this solution is that it can analyze the response of pavement systems in the time domain and can therefore accommodate time-dependent layer properties and incorporate wave propagation. Also, since the back-calculation is performed in the time domain, the algorithm is not sensitive to deflection truncation. The depth-to-stiff layer can also be found, if it exists. The results using simulated deflection time histories and field FWD data showed excellent stability and accuracy. Figure 2 shows the master curve (obtained by shifting all results to reference temperature at 19^{o}C in the x-axis as described in Eqns 1 and 2) for the asphalt layer obtained by using FWD data from two replicate tests (FWD67 and FWD94) for the section PD-21.

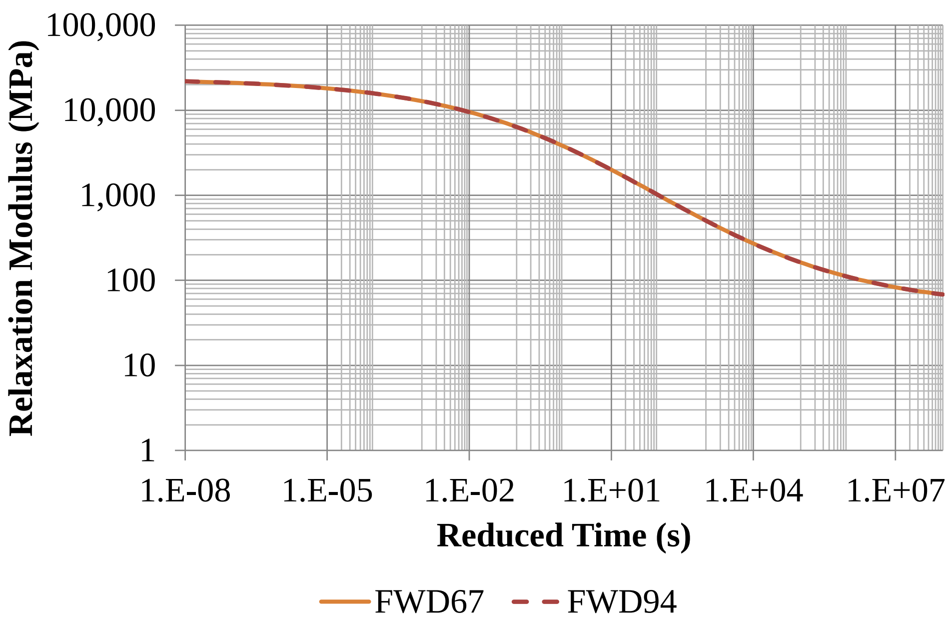

FIGURE 2 Master curve for the asphalt layer obtained by using FWD data for the section PD-21.

Developed master curves were used to calculate model coefficients for the three models. Models were developed by following a factorial design with two speeds, 50km/h and 100km/h, two temperatures, 30^{o}C and 45 ^{o}C, and three vehicle types, car, SUV, and truck for all 17 sections (12 models per section). Average measured layer thicknesses (from iGPR database) and back-calculated stiffnesses for all test sections are given in Table 2.

TABLE 2 Field Tests Sections for Model Development and Fuel Consumption Measurements

Section	L1 type	L1 H (mm)	E1 (MPa)	L2 type	L2 H (mm)	E2 (MPa)	L3 type	L3 H (mm)	E3 (MPa)	L4 type	E4 (MPa)
PD-07	HMA	145	MC	PCC	227	36,000	AB	340	247	SG	181
PD-08	HMA	109	MC	PCC	257	16,000	SG	-	202	-	-
PD-10	HMA	244	MC	PCC	227	11,000	SG	227	147	Stiff	2,000
PD-11	HMA	588	MC	SG	5,000	210	Stiff	-	1,723	-	-
PD-13s1	HMA	395	MC	SG	-	55	-	-	-	-	-
PD-13s2	HMA	379	MC	SG	4,572	83	Stiff	-	3,702	-	-
PD-14	HMA	233	MC	SG	3,086	98	Stiff	-	5,798	-	-
PD-15	HMA	209	MC	SG	-	203	-	-	-	-	-
PD-16	HMA	409	MC	SG	5,207	119	Stiff	-	2,412	-	-
PD-18s1	HMA	180	MC	SG	2,286	114	Stiff	-	689	-	-
PD-18s2	HMA	157	MC	AB	97	172	SG	2,286	114	Stiff	689
PD-19	HMA	610	MC	SG	-	312	-	-	-	-	-
PD-20	HMA	109	MC	CTB	218	288	SG	2,921	74	Stiff	1,654
PD-21	HMA	264	MC	CTB	235	677	SG	-	199	-	-
PD-22s1	HMA	259	MC	AB	452	281	SB	184	590	SG	91
PD-22s2	HMA	341	MC	CTB	130	264	SG	-	92	-	-
PD-23	HMA	237	MC	AB	144	378	SG	-	146	-	-

Note: L1: Layer 1-Top Layer; L1 H: Layer 1 thickness; E1: Layer 1 stiffness; MC: Master curve; PCC: Concrete; AB: Aggregate base; SG: Subgrade: CTB: Cement treated base; SB: Subbase

The load parameters used for OSU and MSU models are given Table 3. Since the MIT model is a viscoelastic beam on an elastic foundation, tire pressure is not used in the analysis. Instead, axle loads shown in Table 3 were used for model development.

TABLE 3 Parameters for Loading for the OSU and MSU Model

Vehicle Class	Number of wheels	Tare Weight (t)	load weight (t)	Tire pressure (kPa)	Load (kN)	Load per tire (kN)	Contact Area (m^2)
Medium Car	4	1.46	0	242	14.308	3.577	0.0148
SUV	4	2.50	0	269	24.500	6.125	0.0230
Heavy truck[1]	8	13.6	21.3	759	302.82	37.853	0.0500

[1] Two tandem axles treated as singles, steering single ignored.

Comparison of Results

Figure 3 shows an example deflection output for the section PD-16 for the truck model. In general for all models, deflection basins from MSU and OSU show similar trends and peaks that are close to each other while the deflection basins calculated by the MIT model are different in shape and magnitude due to the difference in model features (the viscoelastic beam type model subjected to a dynamic load). However, it should be noted that MIT model is calibrated at the fuel consumption level (related to the slope at tire-road contact trajectory and not related to the deflection). Hence the deflection basins shown in Figure 3 are not calibrated quantities and thus would not represent the pavement deflection and are shown only for the sake of completeness. Since the MSU model is an axisymmetric model, the shape of the deflection basin is different from the non-axisymmteric OSU 3D finite element model.

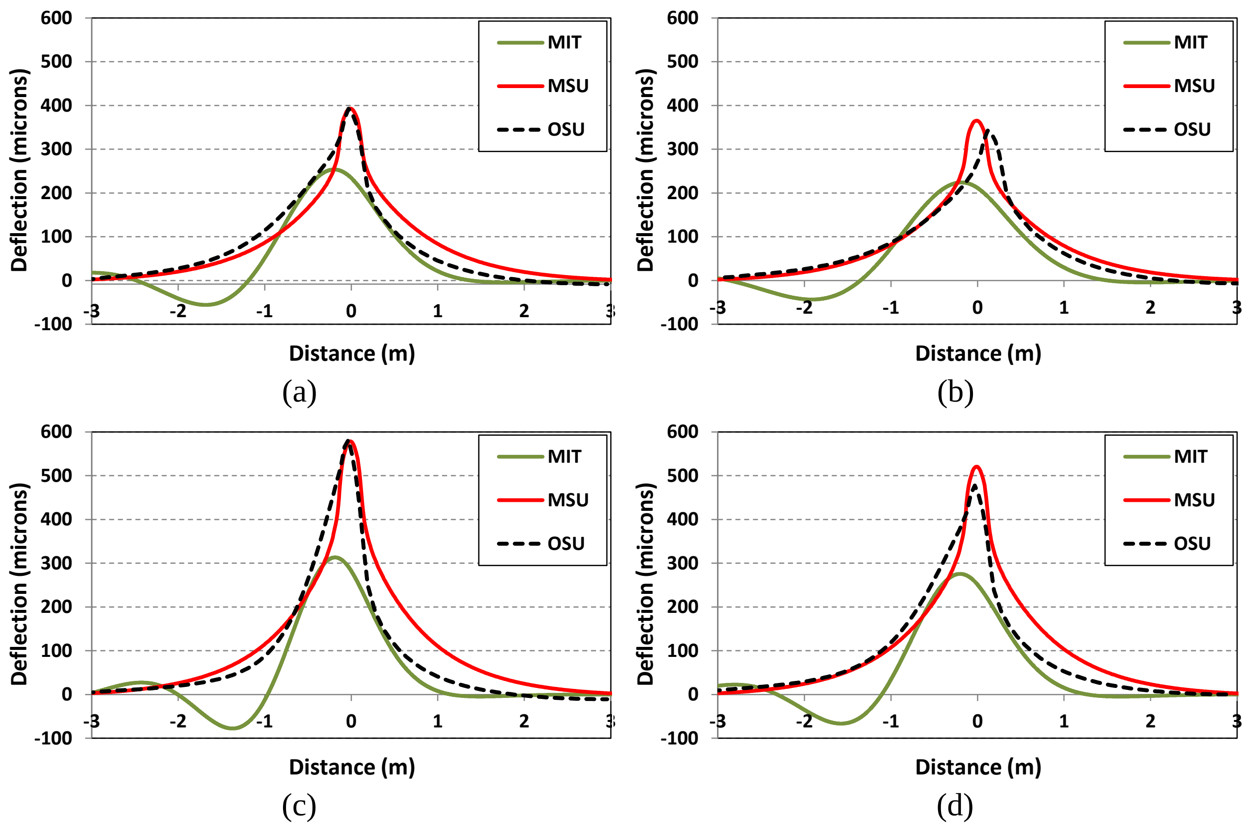

FIGURE 3 Calculated deflection basins for the truck model for section PD-16 (a) Speed (V)=50 km/h, Temperature (T)=30°C, (b) V=100 km/h, T=30°C, (c) V=50 km/h, T=45°C, (d) V=100 km/h, T=45°C.

The MIT and MSU models calculated the dissipated energy based on a wheel moving up slope on the side of the deflection basin. In the OSU model, stress, strain, and phase angle were integrated over time to calculate dissipated energy in the pavement *(5)*. Calculated dissipated energy values by all three models were converted to energy required to make the vehicle move. Finally, EFC (EFC, ml/km) for different vehicles, load levels, and speeds were calculated by dividing the calculated dissipated energy (MJ/km) by the calorific value of the fuel (MJ/L). 10.5MJ/L is used for the calorific value of gasoline (car and SUV) while 16MJ/L is used as the calorific value of diesel for trucks assuming 34.8 MJ/L for gasoline and 30 percent efficiency and 40 MJ/L for diesel and 40 percent efficiency *(2)*.

.

$$excess\ fuel\ consumption\left(\frac{ml}{km}\right) = \frac{W_{truck}}{Fuel\ calorific\left(\frac{MJ}{L}\right)} * 1000 \qquad (11)$$

In this paper, calculated EFC for the following cases are presented: i) Truck-30^{o}C-100km/h (Figure 4a); ii) Car-30^{o}C-100km/h (Figure 4b); iii) Car-45^{o}C-100km/h (Figure 5a); and iv) SUV-45^{o}C-100km/h (Figure 5b) v) Truck-45^{o}C-50km/h (Figure 6a); vi) Truck-45^{o}C-100km/h (Figure 6b);. Results for the complete factorial (12 cases) will be published in a Caltrans report.

Comparison of the predicted EFC for all test sections showed that OSU, MIT, and MSU models produced different results. EFC for OSU and MSU models can be considered to be closer while the MIT model generally predicts a lower EFC. However, observed trends and rankings change for different sections. The primary differences between the MIT model and the other two models are that it assumes deflection of a continuous beam and it does not shear energy dissipation. The current version of the MIT model is also intended to be simplified for producing fast calculations to be used in practical applications, and hence has been noted by the authors to inherently require calibration. To date it has been calibrated with two theoretical cases produced from the finite element model by Pouget et al. (*5*). The other two models use finite elements and includes shear energy dissipation. The relative effects of these differences in the different structures does not yet produce a clear pattern with regard to pavement type (flexible, semi-rigid, composite) or the net effects of the various asphalt materials in the layers in each pavement.

It can be observed from Figure 4 and Figure 5 that EFC values for trucks are about one to two orders of magnitude larger than for cars and SUVs. Although the fuel consumption excess for cars and SUVs are not significant when compared to trucks, higher volume of cars and SUVs on highways can result in significant total car-SUV related EFC in a network level prediction.

Figure 6 shows the effect of vehicle speed on calculated EFC for trucks. In general, changing speed from 100km/h to 50km/h creates a 5% to 35% increase in EFC. Although speed is an important factor affecting the calculated EFC, its effect is less significant when compared to the effects of vehicle type (load effect) and temperature.

By comparing Figure 6b and Figure 4a, it can be observed that increasing temperature from 30^{o}C to 45^{o}C results in 1.1 to 6 times greater EFC. This result suggests that EFC rates start to become more important in summer and in warmer climates.

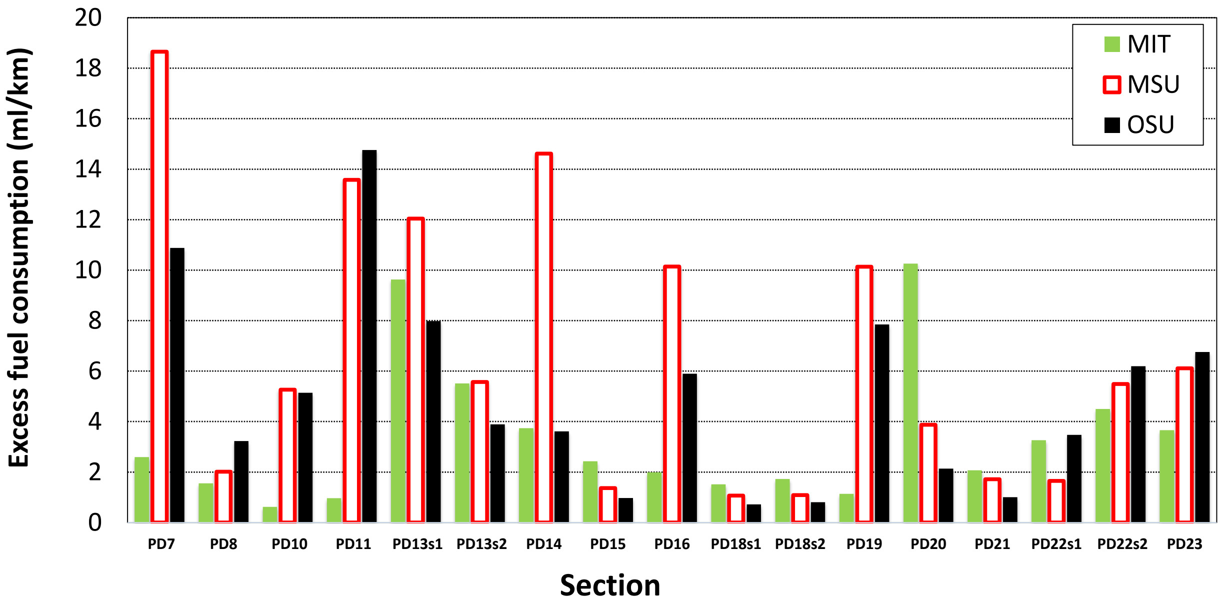

(a)

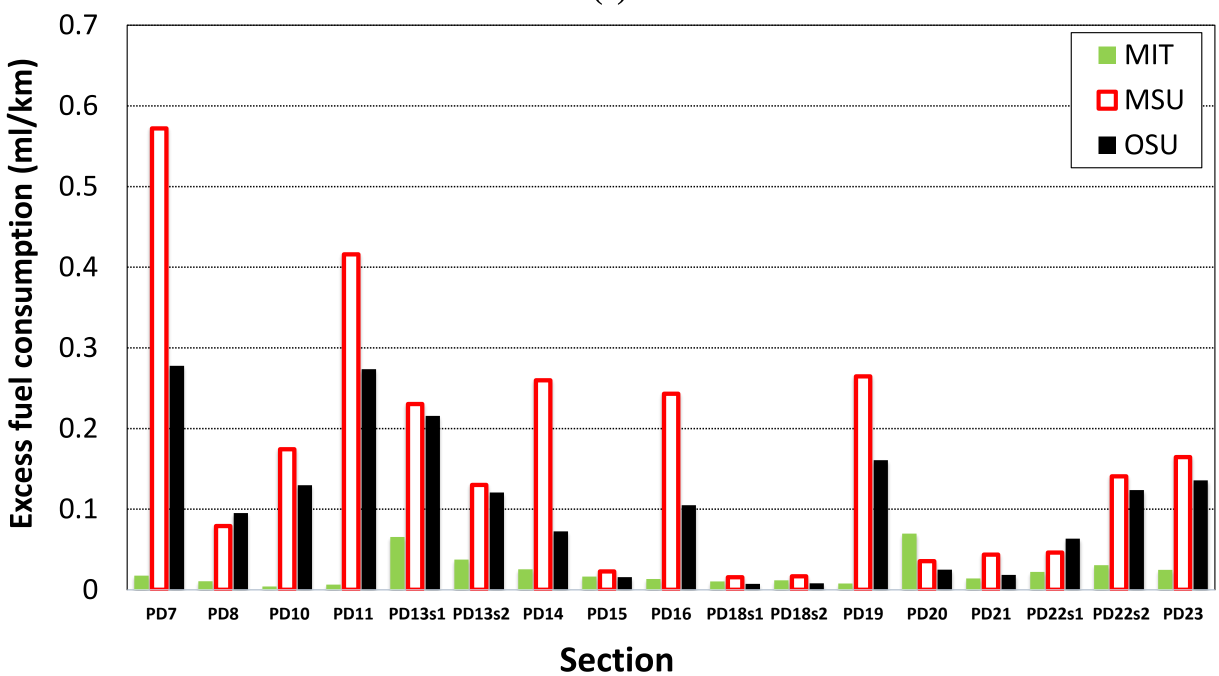

(b)

FIGURE 4 The effect of vehicle type (car and truck) on calculated EFC (a) Truck-30^{o}C-100km/h (b) Car-30^{o}C-100km/h.

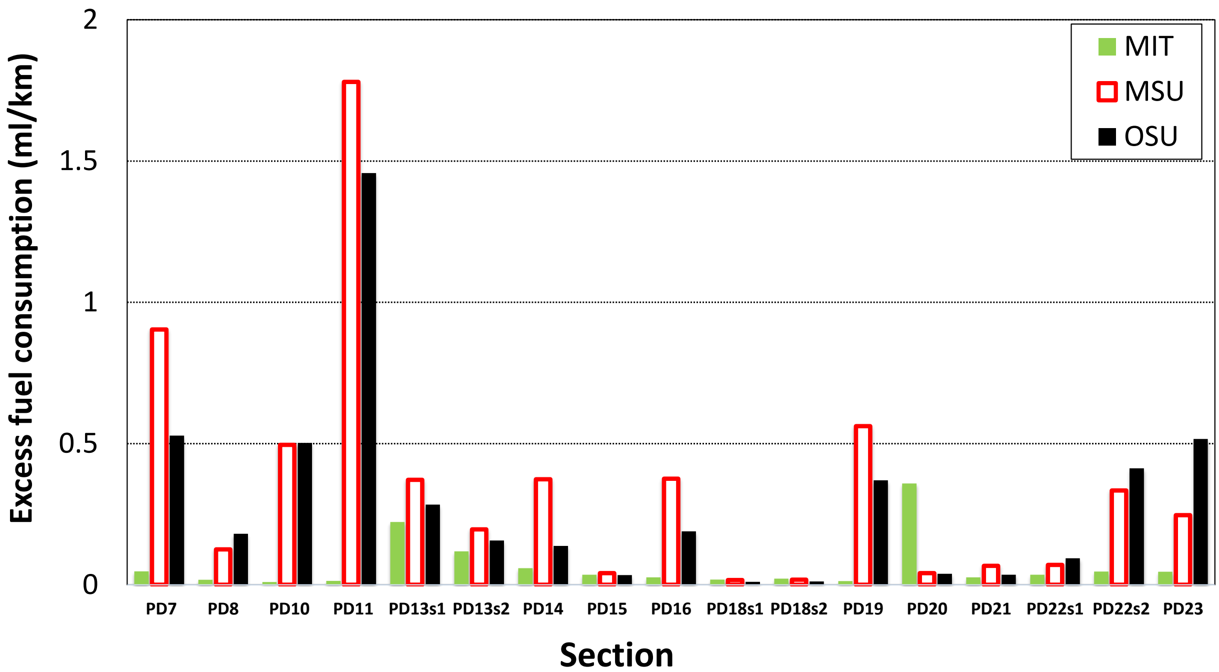

(a)

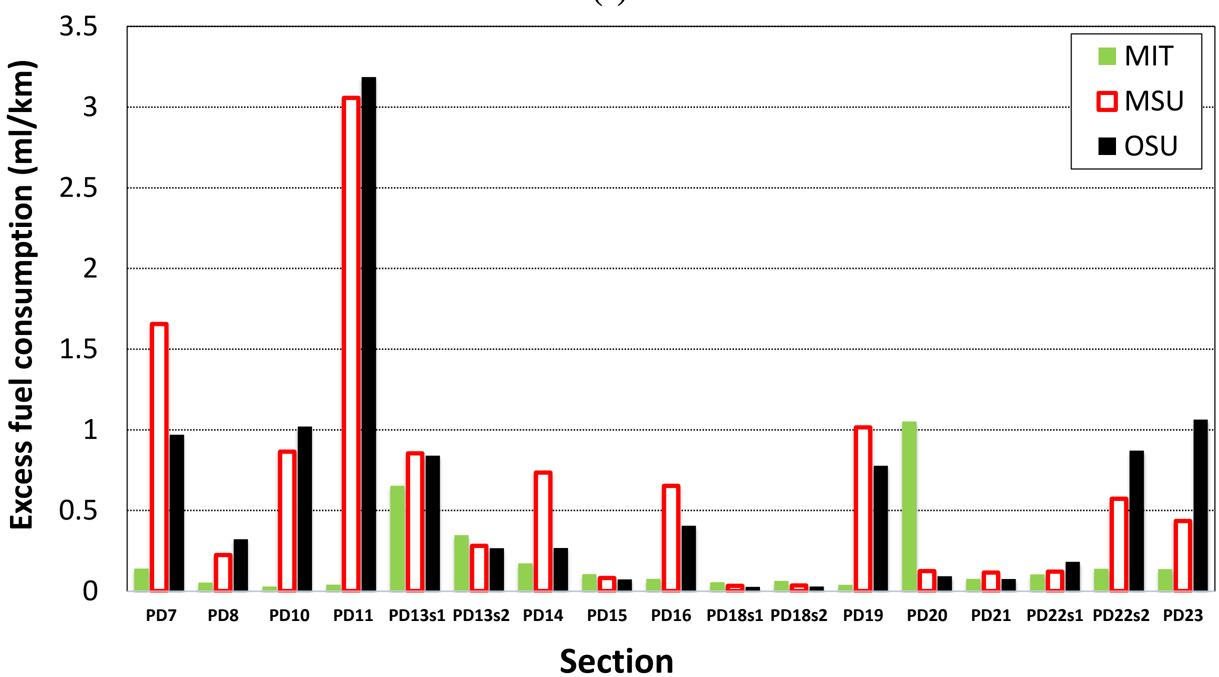

(b)

FIGURE 5 The effect of vehicle type (car and SUV) on calculated EFC (a) Car-45°C-100km/h (b) SUV-45°C-100km/h.

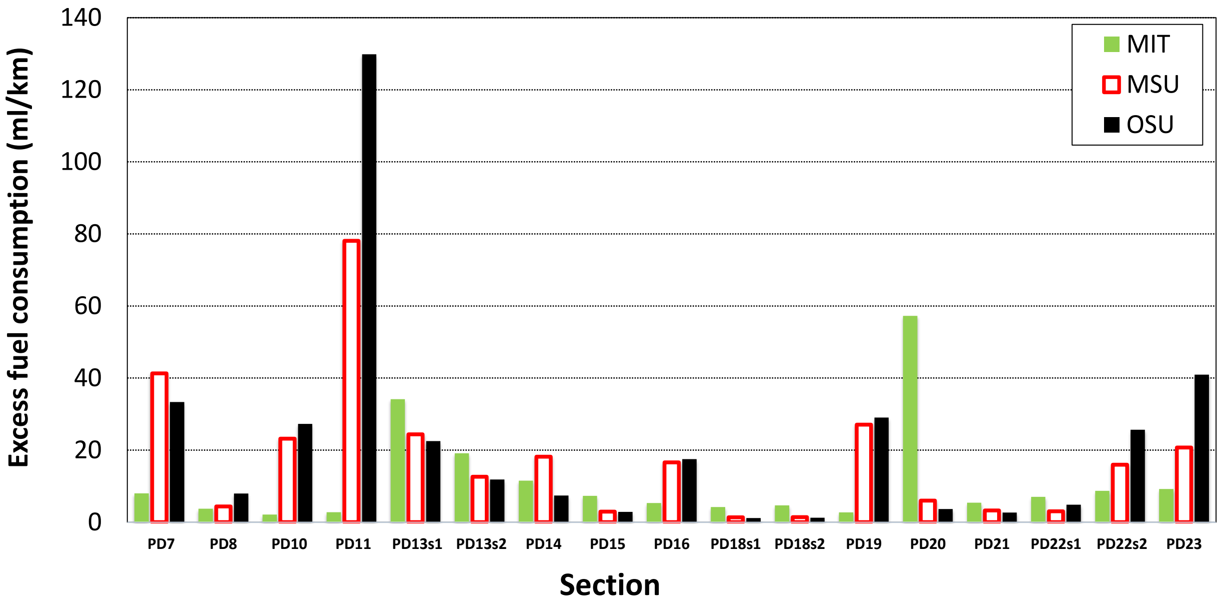

(a)

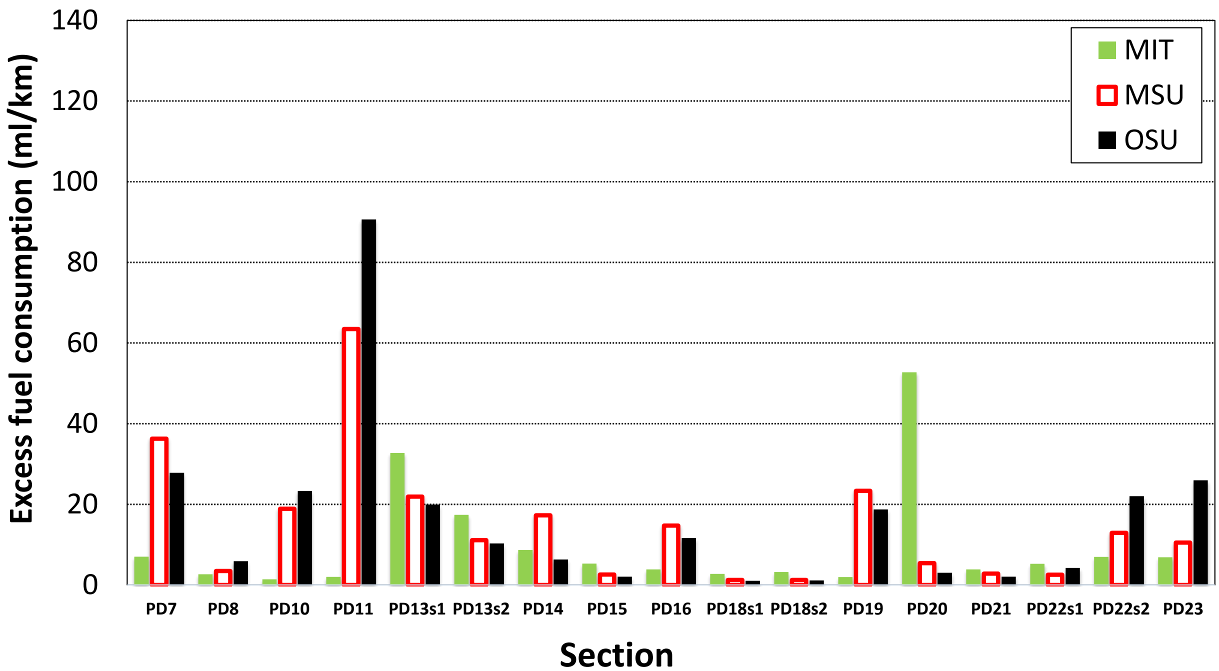

(b)

FIGURE 6 The effect of speed on calculated EFC for trucks (a) Truck-45^{o}C-50km/h (b) Truck-45^{o}C-100km/h.

SUMMARY AND CONCLUSIONS

In this study, consumption of energy due to pavement structural response through viscoelastic deformation of asphalt pavement materials was predicted for 17 field asphalt surfaced sections in California by using three different models. Calculated dissipated energy values were converted to EFC to facilitate comparisons and to be used for network level evaluations. Developed models were used to evaluate the effects of temperature, vehicle speed, and vehicle type (car, SUV, and truck) on viscoelasticity related EFC.

Results of this study can be summarized as follows:

- Comparison of the predicted EFC for all test sections showed that OSU, MIT, and MSU models produced different results. EFC for the OSU and MSU models can be considered to be closer while MIT model generally predicts a lower EFC. The differences between the beam assumption in the MIT model and the OSU and MIT finite element models can likely be attributed to the differences in modeling approach. However, observed trends and rankings change for different sections and no consistent trend can be attributed to a given generic pavement type. The differences within pavement type are most likely due to differences in asphalt mixes, degree of aging and thicknesses, as well as the support provided by the supporting layers. These results indicate that there are important differences within generic pavement types.
- Model predictions are generally of same order of magnitude or an order of magnitude different indicating that overall they can be calibrated using data from field measurements. In general
- In general, deflection basins from MSU and OSU show similar trends and peaks that are close to each other while the deflection basins calculated by the MIT model are different in shape and magnitude. However, it should be noted that MIT PVI model is not intended to provide the deflection basins for pavement sections. The deflection basins shown in this paper are not calibrated and therefore are not representative of pavement deflection.
- Calculated EFC values for trucks are about one to two orders of magnitude larger than cars and SUVs. Although the EFC values for cars and SUVs are not significant when compared to trucks, higher volumes of cars and SUVs on highways can result in significant total car-SUV related EFC in a network level prediction.
- Changing speed from 100km/h to 50km/h creates a 5% to 35% increase in EFC for trucks. Although speed is an important factor affecting the calculated EFC, its effect is less significant when compared to the effects of vehicle type (load effect) and temperature.
- Increasing temperature from 30^{o}C to 45^{o}C results in a 1.1 to 6 times higher EFC for trucks.

The results of this modeling effort will be used in simulations of annual EFC on the field test sections using detailed traffic and pavement temperature hourly distributions. The differences between pavements found in this study are generally of similar order of magnitude as differences between moderately rough and smooth pavement, and the effects of very high macrotexture. Simulations considering traffic speeds, climate, vehicle type and vehicle axle loads are necessary to compare the relative effects of structural response on EFC of different pavements and the effects of roughness and macrotexture. These models were used in simulations that are reported in Reference (*9*).

Once calibrated and validated for the range of pavement included in the study, the full set of models can be used in simplified form for pavement management assessment of the effects of pavement rehabilitation and maintenance on vehicle fuel use and resultant pollutant emissions. They can also be adapted for use in project-level evaluation of alternative designs. In any of these applications agency life cycle cost must be considered in addition to road user cost and environmental impacts.

ACKNOWLEDGMENT

This paper describes research activities that were requested and sponsored by the California Department of Transportation (Caltrans), Division of Research, Innovation and System Information. Federal and State sponsorship and interest are gratefully acknowledged. The contents of this paper reflect the views of the authors and do not necessarily reflect the official views or policies of the Federal Highway Administration or the State of California. This paper does not represent any standard or specification.

REFERENCES

1. Van Dam, T., et al. *Towards Sustainable Pavement Systems: A Reference Document*, Federal Highway Administration, Report FHWA-HIF-15-002, January, 2015.
2. Chatti, K., and Zaabar, I. *Estimating the Effects of Pavement Condition on Vehicle Operating Costs*. Publication NCHRP Report 720. National Cooperative Highway Research Program, Transportation Research Board, 2012.
3. Louhghalam, A., Akbarian, M., and Ulm, F-J. Flügge's Conjecture: Dissipation vs. Deflection Induced Pavement-Vehicle-Interactions (PVI). *Journal of Engineering Mechanics,* 2013, 140 (8), 10.1061/(ASCE)EM.1943-7889.0000754.
4. Louhghalam, A., Akbarian, M., and Ulm, F-J. Scaling Relations of Dissipation-Induced Pavement-Vehicle Interaction. *Transportation Research Record: Journal of Transportation Research Board*, 2014, No.2457, 95-104.
5. Pouget S., Sauzéat C., di Benedetto, H., and Olard, F. Viscous Energy Dissipation in Asphalt Pavement Structures and Implication for Vehicle Fuel Consumption. *Journal of Materials in Civil Engineering*, 2011, 24(5):568-576.
6. Jonsson, P., and Hultqvist, B.Å. *Measurement of Fuel Consumption on Asphalt and Concrete Pavements North of Uppsala*. Swedish National Road and Transport Research Institute, Linköping, Sweden, 2009.
7. Akbarian, M., A. Louhghalam and F.J. Ulm, Mapping the Excess-Fuel Consumption due to Pavement Vehicle Interaction: a Case Study of Virginia's Interstate System, *Papers from the International Symposium on Pavement LCA*, Davis, CA, October, 2014.
8. Sandberg, U. (editor). *Rolling Resistance – Basic Information and State-of-the-Art on Measurement Methods*. Swedish National Road and Transport Research Institute (VTI). Report No. MIRIAM_SP1_01, 2011.

9. Harvey, J., J. D. Lea and C. Kim. *Simulation of Cumulative Annual Impact of Pavement Structural Response on Vehicle Fuel Economy for California Test Sections*. Submitted to the Transportation Research Board, August, 2015.
10. Ferry, J. D. *Viscoelastic Properties of Polymers*. John & Sons, 1980.
11. Yoo, P.J., Al-Qadi, I.L., Elseifi ,M.A., and Janajreh, I. Flexible Pavement Responses to Different Loading Amplitudes Considering Layer Interface Condition and Lateral Shear Forces. *International Journal of Pavement Engineering*, 2006, 7(1):73-86.
12. Bazant, Z.P. Creep and Damage in Concrete. Materials Science of Concrete, J. Skalnet and S. Mindess, eds., *American Ceramic Society*. Westerville, Ohio, 1980, pp 335–389.
13. Stieltjes, T.J., Recherches Sur Les Fractions Continues. *Ann. Fac. Sci. Toulouse (in French)* VIII: 1–122, JFM 25.0326.01, MR 1344720, 1894.
14. Al-Khoury, R., Scarpas, A., Kasbergen, C., and Blaauwendraad, J. Spectral Element Technique for Efficient Parameter Identification of Layered Media. Part I: Forward Calculation. *International Journal of Solids and Structures*. Volume 38. Elsevier, Inc, 2001.
15. Zaabar, I., Chatti, K., and Lajnef, N. Time-Domain Viscoelastic Backcalculation of Pavement Structure Properties from Falling Weight Deflectometer Using Hybrid Approach. In proceedings of *the 3rd International Conference on Transportation Infrastructures - ICTI 2014*, Pisa, Italy, April 22-25, 2014.
16. Louhghalam, A., Tootkaboni, M., and F. J. Ulm. Roughness-Induced Vehicle Energy Dissipation: Statistical Analysis and Scaling. *Journal of Engineering Mechanics*, 2015, 04015046.
17. Louhghalam, A., Akbarian, M., and F. J. Ulm, Roughness-induced pavement-vehicle interactions: Key parameters and impact on vehicle fuel consumption. *Accepted for publication in Transportation Research Record: Journal of the Transportation Research Board*, 2015.